

Research Article





How to cite: Angew. Chem. Int. Ed. **2024**, 63, e202406484 doi.org/10.1002/anie.202406484

Electrochemically Mediated Atom Transfer Radical Polymerization Driven by Alternating Current

Francesco De Bon,* Marco Fantin,* Vanessa A. Pereira, Teresa J. Lourenço Bernardino, Armenio C. Serra, Krzysztof Matyjaszewski, and Jorge F. J. Coelho

Abstract: Alternating current (AC) and pulsed electrolysis are gaining traction in electro(organic) synthesis due to their advantageous characteristics. We employed AC electrolysis in electrochemically mediated Atom Transfer Radical Polymerization (eATRP) to facilitate the regeneration of the activator Cu¹ complex on Cu⁰ electrodes. Additionally, Cu⁰ served as a slow supplemental activator and reducing agent (SARA ATRP), enabling the activation of alkyl halides and the regeneration of the Cu^I activator through a comproportionation reaction. We harnessed the distinct properties of Cu⁰ dual regeneration, both chemical and electrochemical, by employing sinusoidal, triangular, and square-wave AC electrolysis alongside some of the most active ATRP catalysts available. Compared to linear waveform (DC electrolysis) or SARA ATRP (without electrolysis), pulsed and AC electrolysis facilitated slightly faster and more controlled polymerizations of acrylates. The same AC electrolysis conditions could successfully polymerize eleven different monomers across different mediums, from water to bulk. Moreover, it proved effective across a spectrum of catalyst activity, from lowactivity Cu/2,2-bipyridine to highly active Cu complexes with substituted tripodal amine ligands. Chain extension experiments confirmed the high chain-end fidelity of the produced polymers, yielding functional and high molecular-weight block copolymers. SEM analysis indicated the robustness of the Cu⁰ electrodes, sustaining at least 15 consecutive polymerizations.

Introduction

In recent years, alternating current (AC) electrolysis has become a powerful synthetic tool due to its unique oscillating redox environment. In contrast to direct current (DC), which flows in one direction, AC is characterized by a continuous and periodic pulsation or reversal of direction, with the sine wave being the predominant waveform in electric power circuits. Square-wave, triangular wave, sawtooth wave, and pulsed waveforms, as well as combinations of these, have also been used.

Electrosynthesis with AC waveforms may appear to be a niche area, but its properties are extremely attractive. AC has been used in molecular electrosynthesis to influence reaction selectivity,[2] to overcome unwanted side reactions,[3] or to enable new synthesis pathways.[1,3-4] In addition to true AC, pulsed electrolysis (i.e., periodically applying and removing an applied potential or current) can be used to sustain an electrosynthesis reaction.^[5] Recently, we presented and compared how continuous potentiostatic and pulsed electrolysis can affect the electrochemically mediated Atom Transfer Radical Polymerization (eATRP) of common monomers in different solvents on Cu⁰ cathodes. [6] Here, we introduce the use of true AC to drive a polymerization process like electrochemically mediated ATRP, and we investigate the effect of pulse frequency and waveform shape.

ATRP is one of the most used Reversible Deactivation Radical Polymerizations due to its compatibility with various monomers, ability to utilize inexpensive reactants across a wide temperature range, and compatibility with both bulk and monomer/solvent mixtures under homogeneous or heterogeneous conditions. [7] Conventional ATRP uses a large amount of catalyst, which must be removed from the

[*] Dr. F. De Bon, Dr. V. A. Pereira, T. J. Lourenço Bernardino, Prof. A. C. Serra, Prof. J. F. J. Coelho Centre for Mechanical Engineering, Materials and Processes (CEMMPRE), ARISE, Department of Chemical Engineering University of Coimbra Rua Sílvio Lima, Pólo II, 3030-790 Coimbra, Portugal E-mail: francesco@eq.uc.pt Dr. M. Fantin

Dr. M. Fantin
Department of Chemical Sciences
University of Padova
Via Marzolo 1, I-35131 Padova, Italy
E-mail: marco.fantin@unipd.it

Prof. K. Matyjaszewski
Department of Chemistry
Carnegie Mellon University
4400 Fifth Ave, 15213 Pittsburgh, PA, USA
Prof. J. F. J. Coelho

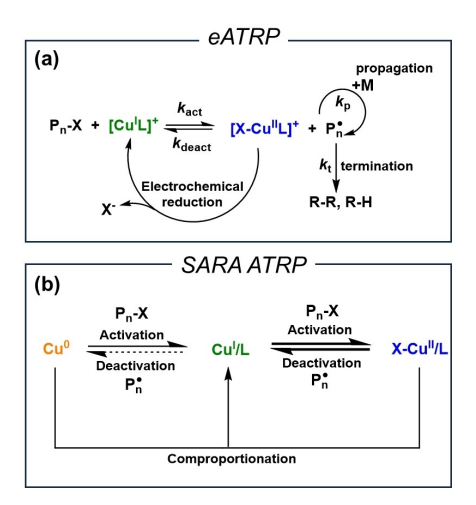
IPN, Instituto Pedro Nunes, Associação para a Inovação e Desenvolvimento em Ciência e Tecnologia Rua Pedro Nunes, 3030-199 Coimbra, Portugal

© 2024 The Author(s). Angewandte Chemie International Edition published by Wiley-VCH GmbH. This is an open access article under the terms of the Creative Commons Attribution License, which permits use, distribution and reproduction in any medium, provided the original work is properly cited.

5213773, 2024, 29, Downloaded from https://onlinelibitary.wiley.com/doi/10.1002/anic.202406484 by Carnegie Mellon University, Wiley Online Library on [03/06/2025], See the Terms and Conditions (https://onlinelibitary.wiley.com/rerms-and-conditions) on Wiley Online Library for rules of use; OA articles are governed by the applicable Creative Commons

polymer by expensive and cumbersome methods. To reduce the catalyst to low part per million (ppm) loadings without compromising polymerization control, new ATRP methods have been developed, including eATRP[8] and supplemental activator and reducing agent (SARA) ATRP[9] (Scheme 1). These methods require active copper catalysts (Cu/L) with large activation rate constant (k_{act}) and ATRP equilibrium constant (K_{ATRP}) . SARA ATRP exploits the comproportionation reaction between Cu^{II} species and Cu⁰ in the presence of free ligand L, to (re)generate Cu^I activator species (Scheme 1a). Cu^I reacts with an initiator or a dormant polymer chain bearing a carbon-halogen bond (P_n-X), to form a propagating radical (Pn •), which adds a few monomer units before being deactivated by the X-Cu^{II}L complex to reform P_n-X. The activation (i.e., radical generation) and deactivation (i.e., radical capping) steps repeat several times until the desired molecular weight is achieved. In addition to promote comproportionation, Cu⁰ can slowly activate P_n-X polymer chain ends. SARA ATRP has been used for various monomers, from (meth)acrylates to vinyl chloride. [9a,c,d,f,10] The method allows temporal control of polymerization as the reaction can be stopped and re-started by lifting and reimmersing a Cu⁰ wire into the polymerization mixture.^[11]

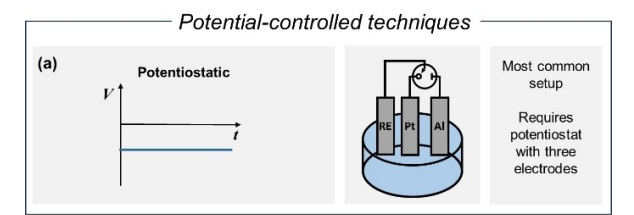
Instead of chemical comproportionation, *e*ATRP directly uses electric current to (re)generate the active Cu^I form of the catalyst (Scheme 1b). The *e*ATRP protocol commonly uses Pt electrodes, but there are environmental advantages in substituting Pt with more abundant metals like Cu. This replacement leads to cost reduction and to savings in electrical charge. ^[6] Cu electrodes not only provide electrons for polymerization initiation but also serve as a supplementary activator and substrate for the regeneration of [Cu^IL]⁺ (SARA ATRP). A Cu—Cu electrode setup is ideal for AC electrolysis. In this symmetrical system, there is no defined anode and cathode as they are indistinguishable at any time during the polymerization due to the rapid change in polarity, according to the frequency of the waveform (*f*).

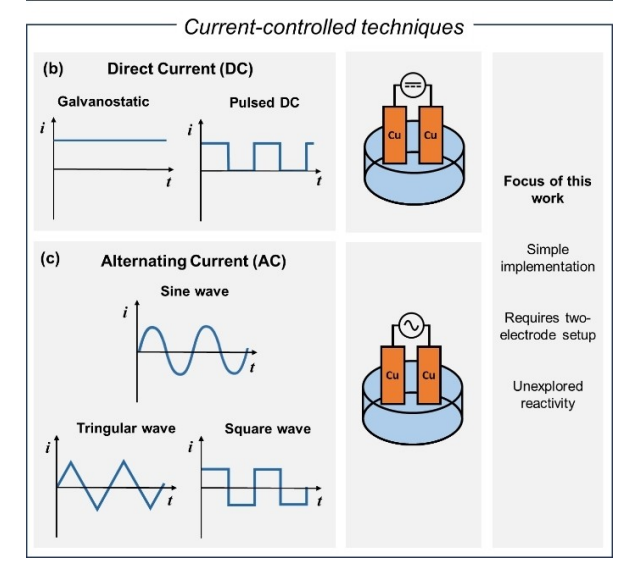


Scheme 1. Mechanism of copper-catalyzed (a) eATRP and (b) SARA ATRP. In SARA ATRP bold lines indicate the main reaction routes.

Conventional eATRP is typically potentiostatic (i.e. fixed potential, $E_{\rm app}$) or galvanostatic (i.e. fixed current, I_{add}). [8c,e] Typical electrosyntheses setup are shown in Scheme 2. Potentiostatic eATRP requires the use of a potentiostat and a three-electrode setup, including a reference electrode (RE). In contrast, current-controlled method requires only two electrodes (working and counter electrodes), but they are often less selective. A common problem with galvanostatic electrolysis is that, to maintain a fixed current, the electrode potential changes during the experiment. The uncontrolled potential can lead to slow reactions or excessive side reactions, which has been observed in eATRP on Pt/Pt or Pt/Al electrode pairs, as well as in other organic electrosynthesis. [6,12] The typical solution to this problem is to perform galvanostatic eATRP with multiple, carefully optimized current steps,[13] which increases complexity.

Here instead we use a single current step/value to perform eATRP with pulsed and AC controlled techniques (Scheme 2). First, we evaluated the performance of the DC techniques by comparing galvanostatic and pulsed electrolysis at different pulse frequencies. We then focused only on AC eATRP operated with different wave functions (sine, triangular, and square wave). AC eATRP is finally applied to prepare linear and block copolymers of multiple monomer classes (acrylates, styrene, and functional monomers). The unique oscillating redox environment of AC ATRP





Scheme 2. Scheme of electrochemical techniques applicable to *eATRP*: (a) potentiostatic (DC electrolysis), (b) galvanostatic (DC electrolysis) and (c) alternating (AC electrolysis with Cu⁰ electrode setup, *this work*).

5213773, 2024, 29, Downloaded from https://onlinelibary.wiley.com/doi/10.1002/anie.022406484 by Carnegie Mellon University, Wiley Online Library on [03/06/2025]. See the Terms and Conditions (https://onlinelibrary.wiley.com/terms-and-conditions) on Wiley Online Library for rules of use; OA articles are governed by the applicable Creative Commons License and Conditions (https://onlinelibrary.wiley.com/terms-and-conditions) on Wiley Online Library for rules of use; OA articles are governed by the applicable Creative Commons License and Conditions (https://onlinelibrary.wiley.com/terms-and-conditions) on Wiley Online Library for rules of use; OA articles are governed by the applicable Creative Commons License and Conditions (https://onlinelibrary.wiley.com/terms-and-conditions) on Wiley Online Library for rules of use; OA articles are governed by the applicable Creative Commons License and Conditions (https://onlinelibrary.wiley.com/terms-and-conditions) on Wiley Online Library for rules of use; OA articles are governed by the applicable Creative Commons License and Conditions (https://onlinelibrary.wiley.com/terms-and-conditions) on Wiley Online Library for rules of use; OA articles are governed by the applicable Creative Commons License and Conditions (https://onlinelibrary.wiley.com/terms-and-conditions) on Wiley Online Library for rules of use and the use of use and use and

proved to be very versatile for the synthesis of functional homo- and block-copolymers.

Monomers N MA BA EHA AN N N H AN NIPAM NIPAM OEOMA500

Scheme 3. Structures of monomers, initiators, and Cu ligands used in this work.

Results and Discussion

Optimization of Reaction Conditions under Direct and Pulsed Current

We first focused on the Cu^{II}Br/TPMA-(PYR)₃ catalyst (Scheme 3), a highly active catalyst with three electrondonating groups (EDGs) in the para positions of the tripodal pyridine ligand. We performed eATRP of methyl acrylate (MA) by reducing 0.3 mM Cu^{II}Br/TPMA-(PYR)₃ by pulsed electrolysis on a Cu/Al electrode pair, with Cu as working electrode (WE) and Al as sacrificial counter electrode (CE). During pulsed DC, the cell state transitioned from an open cell condition (no applied electrochemical stimulus) to a small current of $-18\,\mu\text{A}$ (this current corresponds to I_{ave} , the average current determined from the charge passed during a model potentiostatic electrolysis, $I_{\text{ave}} = |Q|/t$, see Figure S3b). After application of the pulsed waveform, a well-controlled ATRP was triggered, achieving a conversion > 50% in 2 hours, with D=1.11 and the experimental molecular weights agreeing quite well with the theoretical values (Entry 1, Table 1).

Our first experiments aimed to select the ideal electrode material by comparing Cu vs Al anodes, maintaining a constant total Cu area of 4.4 cm² to ensure a constant contribution from comproportionation reactions (Entries 1–2, Table 1). The utilization of a Cu⁰ anode enabled a faster and better controlled polymerization, possibly due to the release of additional Cu^I activator complex from Cu⁰ during the oxidation step (see below). To further improve conversion, we completely removed the initial amount of CuII deactivator in the solution and observed a significant increase in conversion (from 60 % to 84 %, Entry 4, Table 1). The excellent retention of D, even without the initial amount of Cu added, demonstrates that [BrCu^{II}TPMA–(PYR)₃]⁺ is a fast deactivator and overall an excellent catalyst for low ppm eATRP with pulsed electrol-

Entries 3–6 in Table 1, as well as Figure 1a, b illustrate the effects of the frequency (f) of pulsed electrolysis on Cu/Cu electrodes, ranging from 0 (i.e., galvanostatic, no pulse) to 10 Hz. The galvanostatic process (f=0 Hz, single step of $I_{\rm app}$ = $-18\,\mu{\rm A}$, Entry 7, Table 1) resulted in a

Table 1: eATRP of 50 vol% MA catalyzed by $[Br-Cu^{II}TPMA-(PYR)_3]^+$ in DMSO + 0.1 M Et_4NBF_4 at $T=40^{\circ}C$. $I_{app}=-18~\mu A$ (during pulse), t=2~h.

$Entry^{[a]}$	DC Mode	f (Hz)	Electrodes	$C^0_{[Cu^{11}L]^{2+}}$ (mM)	$k_{p}^{app} (h^{-1})^{[b]}$	Conv. (%) ^[c]	$M_{\rm n}^{\rm GPC} \times 10^{-3[d]}$	$M_{\rm n}^{\rm th} \times 10^{-3[e]}$	I_{eff}	$\mathcal{D}^{[f]}$
1	Pulsed	0.1	Cu/Al	0.3	0.38	52	28.3	24.9	0.88	1.11
2	Pulsed	0.1	Cu/Cu	0.3	0.46	60	32.6	28.5	0.87	1.06
3	Pulsed	0.01	Cu/Cu	0	0.50	61	32.7	29.5	0.90	1.06
4	Pulsed	0.1	Cu/Cu	0	0.92	84	39.4	40.2	1.02	1.06
5	Pulsed	1	Cu/Cu	0	0.50	57	32.7	27.6	0.85	1.06
6	Pulsed	10	Cu/Cu	0	0.66	64	32.9	30.7	0.92	1.04
7	Galvanostatic	0	Cu/Cu	0	0.90	78	49.3	37.1	0.75	1.12
8	None (SARA ATRP)	-	Cu/Cu	0	0.33	45	45.1	21.4	0.47	1.15

[a] Other conditions: MA/EBiB/TPMA-(PYR) $_3$ = 552/1/0.09; C_{MA} = 5.52 M in DMF + 0.1 M Et $_4$ NBF $_4$, EBiB = ethyl α -bromoisobutyrate initiator, T = 40 °C, V_{tot} = 15 mL; activated Cu wire: area = 4.4 cm² (Entry 1) or 2×2.2 cm² (Entries 2–7); stirring rate = 700 rpm. [b] Calculated as the slopes of $ln([M]_0/[M]) \nu s t$ plots. [c] Calculated from 1 H NMR in CDCl $_3$ using DMF as internal standard. [d] Calculated from THF GPC with triple detector at T = 30 °C. [e] Calculated from 1 H NMR: M_n th = Conv.×DP× M_{MA} + M_{EBiB} . [f] D = M_w/M_n .

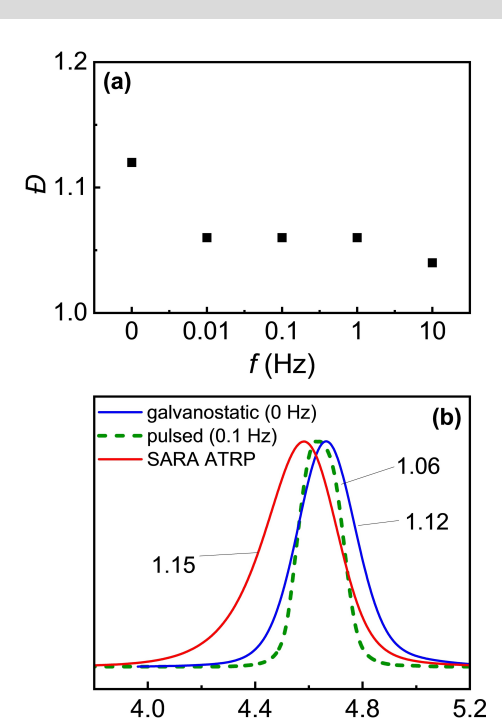


Figure 1. (a) Dispersity as a function of pulse frequency. (b) Comparrison of GPC traces after 2 h for galvanostatic (blue), 0.1 Hz pulsed electrolisys (green), and SARA ATRP (red line). Dispersity values are labeled on the curves.

log M

polymerization of comparable rate to the pulsed processes and faster than SARA ATRP, but PMA had dispersity higher than the pulsed process (yet still of low D = 1.12). An intermediate pulse frequency (f=0.1 Hz) led to the most favorable results, showing fast kinetics, and producing PMA-Br with very low D. It should be noted that the pulsed processes used half the charge of the galvanostatic process, but results in equally fast polymerization. In contrast, polymerizations were slower at higher frequencies (f>1 Hz, Entry 5-6, Table 1). The higher frequencies did not affect D (i.e., deactivation remained fast and effective, Figure 1b). Overall, this points to a diminished activation process at higher f, where the electrochemical reduction (Faradaic process) is partially hindered by the continuous and rapid charging and discharging of the bilayer interface (capacitive processes), which leads to a waste of ca. 10 % of electrical charge (see calculation in Supporting Information, Figure S23). Finally, a control experiment with no applied current (i.e., SARA ATRP, Entry 8, Table 1) provided a slower polymerization and PMA was slightly more dispersed and with poorer molecular weight control than pulsed or galvanostatic eATRP. This SARA control experiment confirmed the role of Cu⁰ as slow supplemental activator and reducing agent. Figure 1b highlights the lower dispersity of the pulsed electrolysis (f=0.1 Hz) compared to the SARA ATRP or galvanostatic (f=0 Hz) electrolysis processes.

eATRP with Real AC Electrolysis on Cu/Cu Electrode Pair

Having established that f=0.1 Hz is optimal for efficient polymerizations, we investigated eATRP triggered by a setup that generates true AC waveforms. Unfortunately, common potentiostats do not provide real AC electrolysis with sinusoidal or triangular waves, only square waves are supported. On the other hand, inexpensive laboratory-grade AC wavefunction generators (which are ca. 10 times less expensive than common potentiostats) can be used to produce real sinusoidal wavefunctions. The electrochemical setup is schematically drawn in Figure 2a and described in detail in the Supporting Information. The electrochemical cell comprised two Cu0 wires immersed in the polymerization mixture (Figure 2b). Due to the symmetrical Cu/Cu system, there was no distinction between anode and cathode when the polarity was changed. Notably, a reference electrode was unnecessary, which simplified the setup. We investigated three AC waveforms (sinusoidal, triangular, and square wave) and compared them to a polymerization driven by a linear waveform (DC, corresponding to f=0 Hz). To provide meaningful comparison with the pulsed electrolysis presented in Table 1, the AC root-meansquare (rms) current was monitored via oscilloscope and set to $I_{\rm rms} = 22 \,\mu{\rm A}$ at a frequency $f = 0.15 \,{\rm Hz}$ (slight differences to the conditions of Table 1 are due to instrumental limitations). The results in Table 2 and Figure 3 show that, in all cases, AC eATRPs had similar rates to DC eATRP but faster than SARA ATRP performed in the same medium. Each alternating waveform improved the control of PMA-Br. Among the waveforms, the sine and square wave proved to be the best: both provided high conversions in a short time, and PMA-Br showed remarkable control (D=1.03-1.06). Overall, AC electrolysis performed similarly to a pulsed electrolysis (0.1 Hz, Table 1, entry 4).

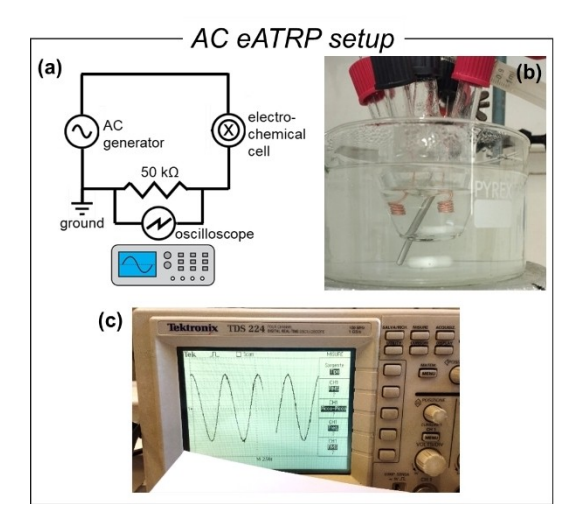


Figure 2. (a) Scheme of the electric circuit used for real AC electrolysis, (b) digital picture of the electrochemical cell used and (c) of the oscilloscope showing the sinusoidal wave sent to the electrochemical cell during galvanostatic AC eATRP of 50 vol % MA.



Angewandte

Table 2: AC eATRP of 50 vol% MA catalyzed by $[Cu^{II}TPMA-(PYR)_3]^{2+}$ in DMSO+0.1 M Et_4NBF_4 at $T=40^{\circ}C$; $C_{Lfree}^0=0.9$ mM and no initial Cu^{II} , $I_{\rm rms} = 22 \, \mu A$.

Entry ^[a]	Waveform	f (Hz)	Peak current (µA)	t (h)	Conversion (%) ^[b]	$k_{\rm p}^{\rm app} \ ({\rm h}^{-1})^{\rm [c]}$	$M_{\rm n}^{\rm GPC} \times 10^{-3[d]}$	$M_{\rm n}^{\rm th} \times 10^{-3[e]}$	I_{eff}	$\mathcal{D}^{[g]}$
1	Linear (DC)	0	22	3	82	0.90	38.3	39.2	1.02	1.15
2	Sinusoidal	0.15	32	2	77	0.89	43.4	37.2	0.86	1.03
3	Triangular	0.15	44	2	73	0.79	38.7	35.2	0.91	1.11
4	Square	0.15	22	2	75	0.76	42.0	36.0	0.86	1.06

[a] Other conditions: MA/EBiB=552/1; C_{MA} =5.52 M in DMSO+0.1 M Et₄NBF₄, T=40°C; activated Cu⁰ wires: I=2×7 cm; stirring rate=700 rpm. [b] Calculated from 1 H NMR in CDCl₃ using DMF as internal standard. [c] Calculated as the slopes of $\ln([M]_0/[M]) \nu s t$ plots. [d] Calculated from THF GPC with triple detector at $T=30\,^{\circ}$ C. [e] Calculated from 1 H NMR: $M_n^{th}=\text{Conv.}\times\text{DP}\times M_{MA}+M_{\text{EBiB}}$. [g] $D=M_w/M_n$.

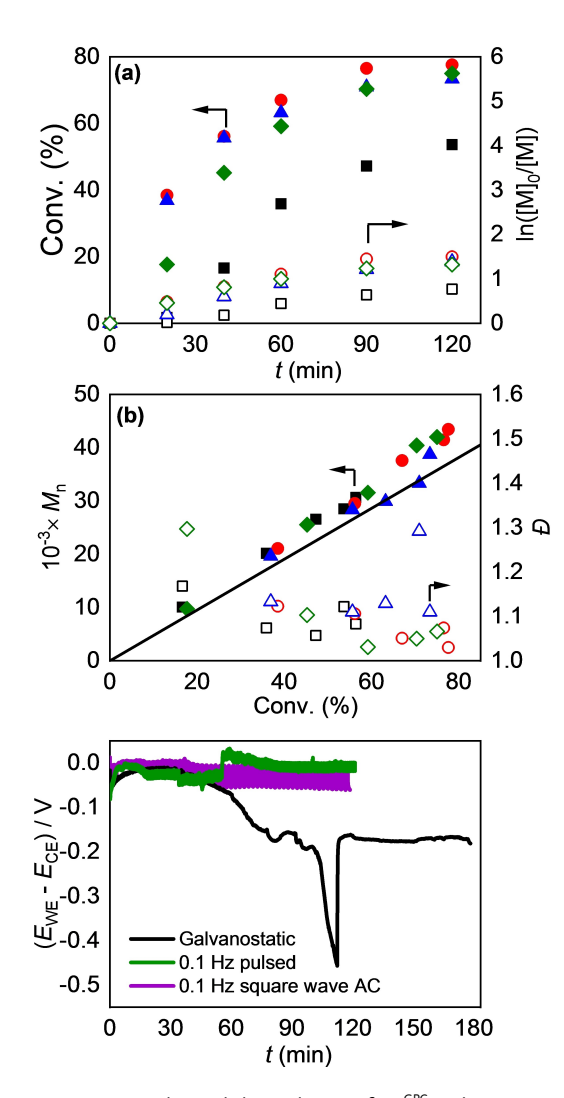


Figure 3. (a) Kinetic plot and (b) evolution of M_n^{GPC} and $\mathfrak D$ vs conversion recorded during the AC eATRP of 50 vol % MA in DMSO + 0.1 M Et₄NBF₄ using various waveforms at f= 0.15 Hz at T= 40 $^{\circ}$ C using [Cu^{II}TPMA-(PYR)₃]²⁺ as catalyst and Cu⁰ electrodes. Symbols: (\blacksquare) linear at f=0 Hz; (\bullet) sinusoidal, (\triangle) triangular and square wave (*) using f=0.15 Hz. The black straight line in b) corresponds to the theoretical molecular weight. (c) Potential difference between WE and CE during galvanostatic, pulsed, and square-wave AC (0.1 Hz).

Although each AC wave had the same I_{rms} (22 μ A) there were differences in the peak currents (I_p) due to the shape of the waves. Peak current in the triangular waveform was

 $\pm 44 \,\mu\text{A}$, twice the value of the square wave $(I_p = I_{\text{rms}} =$ 22 µA). The twice higher peak current of the triangular waveform may justify the slightly higher D in this case, due to too high peak concentration of Cu(I) activators on the electrode surface.

Figure 3c shows the potential difference between the two electrodes during AC and galvanostatic processes. The potential difference continuously increased in the galvanostatic process, until 120 min when a discontinuity was observed, and the polymerization stopped. Conversely, much lower potential differences were observed in both pulsed and square wave electrolyses. This indicates that pulsed polarity switching is more efficient than the continuous reduction process at the same electrode (galvanostatic).

AC eATRP of Different Monomers: Wide Applicability and Scalability

We expanded the applications of AC eATRP to polymerize additional monomers and to scale up the reaction. Typically, lengthy process optimization steps have been necessary to identify suitable eATRP conditions for new monomers. These steps involved studying the applied potential, followed by the development of a customized galvanostatic process (i.e., applying a current profile), usually with multiple current steps. Instead, the distinctive oscillating redox environment of AC eATRP demonstrated broad applicability, surpassing that of potentiostatic and galvanostatic eATRP methods reported thus far. In particular, the same square wave electrolysis conditions ($I_p = \pm 18 \,\mu\text{A}$ and f=0.15 Hz) were applied to polymerize eight monomers in addition to MA, including methyl methacrylate (MMA), acrylonitrile (AN), 2-ethylhexyl acrylate (EHA), 2-methacryloyloxyethyl trimethylammonium chloride (METAC), Nisopropylacrylamide (NIPAM), styrene (Sty), n-butyl acrylate (BA), and acrylamide (AAm), in three common solvents (DMSO, DMF, H₂O and in bulk) and with four different ATRP catalysts (see Table 3 and Scheme 3) selected to match the reactivity of the polymeric chain ends. For example, high activity Cu/TPMA-(PYR)₃ was used for less active polyacrylate chain ends, while low-activity Cu/ bpy was used for more reactive polymethacrylate and polyacrylonitrile chain ends. Additionally, the AC eATRP of BA and AAm have been carried out at a larger scale of 100 mL, maintaining the same frequency of 0.15 Hz, and

Table 3: AC eATRP of different monomers at f=0.15 Hz with a squarewave: $I_{p-p}=\pm 18$ μA for small scale experiments (15 mL) and $I_{p-p}=\pm 363$ μA for large scale experiments (100 mL).

Entry	Monomer	Ligand	Solvent	t (h)	Conversion (%) ^[c]	$k_{\rm p}^{\rm app} \ ({\rm h}^{-1})^{[{\rm d}]}$	$M_{\rm n}^{\rm GPC} \times 10^{-3[e]}$	$M_n^{th} \times 10^{-3[f]}$	I_{eff}	$\mathcal{D}^{[\mathrm{g}]}$
Small s	cale (15 mL),	I _{p-p} = ±18 μΑ								
1 ^[h]	MA	TPMA-(PYR) ₃	DMSO	2	75	0.76	42.0	36.0	0.86	1.06
2 ^[i]	MMA	Вру	DMSO	3	61	0.32	32.8	28.7	0.88	1.09
3 ^[f]	AN	Вру	DMSO	4	91	0.45	47.3	37.5	0.79	1.02
[^[k]	EHA	TPMA-(PYR) ₃	DMF	2.5	89	0.88	40.1	39.4	0.98	1.40
[[]	METAC	TPMA	H ₂ O	3	78	0.55	47.2	39.1	0.83	1.21
[m]	NIPAM	Me ₆ TREN	H₂O	4	98	0.84	52.8	49.7	0.94	1.04
7 [n]	Sty	PMDETA	Bulk	8	18	0.02	21.4	16.2	0.76	1.12
Large s	cale (100 mL)	, I _{p-p} = ±363 μA								
3 ^[0]	BA	Me ₆ TREN	DMF	4	90	0.36	39.9	40.6	1.02	1.03
) [p]	AAm	Me ₆ TREN	H₂O	3	93	0.97	53.6	46.7	0.87	1.09

utilizing the same electrode pair (surface area = 4.4 cm²), with the only difference being the adjustment of I_p to $\pm 363 \,\mu\text{A}$. This adjusted I_{p} was derived from published formulas using the surface area of the electrodes and the reaction scale-up factor. [8a] Relatively fast polymerizations were observed in all cases, with conversions up to 90 % for most monomers. Quantitative conversion was observed for acrylamides at a small scale (NIPAM), and 93 % at a large scale (AAm). We observed very low dispersity (1.02 for PAN, 1.03 for PBA at a 100 mL scale, and 1.04 for PNIPAM). The highly hydrophobic PEHA exhibited a higher dispersity of 1.40, attributed to poor polymer solubility in DMF at high conversions. Notably, we successfully polymerized styrene in bulk. This monomer, being rather non-polar, presents challenges due to its high electrochemical resistance. However, thanks to the relatively large surface area of the electrodes, the low currents used in AC eATRP, and the more hydrophobic supporting electrolyte tetrabutylammonium tetrafluoroborate, we achieved a slow but satisfactory polymerization.

These results show that eleven monomers (including 2-hydroxyethyl acrylamide and poly(ethylene glycol) methyl ether methacrylate used in chain-extension experiments) can be polymerized with the same electrochemical protocol. This contrasts to previous reports of eATRP, which required extensive optimization procedures for each monomer. AC eATRP is also compatible with the entire range of catalyst activity, from the low-activity catalyst Cu/2,2-bipyridine to Cu/TPMA—(PYR)₃, the most active catalyst known to date. This highlights the broad versatility of AC eATRP for a wide range of monomers, catalysts, and initiators, up to a scale of 100 mL in organic solvents, water, and bulk.

Modulation of Molecular Weight in AC eATRP

AC eATRP was further investigated for modulating the molecular weights of PBA–Br (Table S5). The targeted degree of polymerization (DP_T) was increased from 349 to 3490 by adjusting the initiator concentration ($C_{\rm EBiB}$). AC eATRP permitted to synthetize PBA–Br up to $M_{\rm n}^{\rm GPC}$ = 223,000. Conversions were high (~90%) for DP_T=349–698 and decreased when targeting higher DP_T. The molecular weights were in good agreement with theoretical values, with relatively low dispersity (D=1.04–1.31). This demonstrates the high degree of control over the synthesis of polymers with varying molecular weights.

Chain-End Fidelity

To confirm the chain-end fidelity of the polymers synthesized by AC eATRP, we performed three chain extension experiments for three representative monomer classesmethacrylates, acrylamides, and acrylates. Notably, all polymerizations were triggered by AC eATRP under the same conditions, utilizing a square waveform and $I_p = 22 \,\mu\text{A}$ at the same Cu^0 electrode pair PMETAC-Cl $(M_n^{GPC} =$ 50,500, D=1.20) was first synthesized using $[Cu^{II}TPMA]^{2+}$ as catalyst, and then used as a macroinitiator for chain extension with poly(ethylene glycol) methyl ether methacrylate (OEOMA500). The resulting block copolymer had a molecular weight $M_{\rm n}^{\rm GPC} = 116,000$ and a low D = 1.23. In addition, the GPC traces were clearly shifted to a higher MW region without tailing or shoulder peak in the lower MW region (Figure 4b). A similar phenomenon was observed when a PNIPAM-Br macroinitiator $(M_n^{app} =$ 56,000, D=1.04) was synthetized with $[Cu^{II}Me_6TREN]^{2+}$ and extended with N-hydroxyethyl acrylamide (HEAAm),

Figure 4. (a) Chain extension experiments via AC eATRP. Molecular weight distribution of macroinitiator and block copolymer obtained during the chain extension: (b) PMETAC-b-P(OEOMA₅₀₀)-Cl, (c) PNIPAM-b-PHEAAm-Br; (d) PMA-b-PMA-Br. SEM images of the electrode surface (e) before and (f) after 15 AC eATRPs. The white bar in (e) and (f) represents a scale of 100 µm.

yielding PNIPAM–*b*–PHEAAm–Br ($M_n^{\rm app}$ =113,000 and D=1.06, Figure 4c). Finally, a chain extension of a PMA–Br macroinitiator ($M_n^{\rm GPC}$ =37,600, D=1.05) with fresh MA, targeting high molecular weights, produced the pseudoblock copolymer PMA–*b*–PMA–Br ($M_n^{\rm GPC}$ =591,000, D=1.46) and confirmed the high livingness of this macroinitiator prepared in DMSO (Figure 4d).

Reusing Cu⁰ Electrodes

We assessed the reusability of the Cu⁰ wires as electrodes for AC *e*ATRP. While Cu⁰ electrodes are cost-effective compared to Pt, it is unreasonable to replace them after each polymerization. Therefore, we analyzed the surface condition of the electrodes before and after conducting 15 AC eATRPs (including all experiments of Tables 4, Table S4, as well as all chain extension experiments). SEM

analysis revealed only minor surface changes after the polymerization cycles (Figure 4d and Figure S27–28), and there was no observed decline in performance. The electrode pair could be used for at least 15 consecutive reactions by simply activating/renovating the surface through immersion in an HCl/MeOH cleaning solution. This also highlights the minimal impact of the small oxidative AC currents when the electrodes function as anodes.

Mechanistic Investigations

The cathodic reaction in eATRP is the reduction of Cu(II) to Cu(I). However, the inversion of polarity in AC eATRP raises the question of what reaction takes place at the Cu electrode during the oxidation step. To investigate this aspect, we conducted cyclic voltammetry on a Cu^0 disk electrode in DMSO (Figure 5a).

Table 4: AC eATRP of 50 vol % MA catalyzed by $[Cu^{II}L]^+$ in DMSO + 0.1 M Et₄NBF₄ at $T=40\,^{\circ}C$; $C_{L,free}^0=0.9$ mM and no initial Cu^{II} , f=0.15 Hz after 1.5 h of reaction time.

Entry ^[a]	Ligand	E _{1/2}	$\log k_{\rm act}^{\rm [b]}$	Conversion (%) ^[s]	$k_{\rm p}^{\rm app} \ ({\rm h}^{-1})^{\rm [d]}$	$M_{\rm n}^{\rm GPC} \times 10^{-3[e]}$	$M_n^{\text{th}} \times 10^{-3[f]}$	I_{eff}	$\mathcal{D}^{[\mathrm{g}]}$
1	TPMA	-0.227	2.3	59	0.69	29.8	32.8	1.10	1.10
2	Me ₆ TREN	-0.342	3.3	61	0.73	21.9	28.9	1.32	1.09
3	TPMA-(PYR) ₂	-0.416	4.1	77	1.02	44.2	36.7	0.83	1.05
4	TPMA-(PYR) ₃	-0.481	4.8	77	1.05	41.5	36.7	0.88	1.07

[a] Other conditions: MA/EBiB=552/1; C_{MA} =5.52 M in DMSO+0.1 M Et₄NBF₄, T=40°C; activated Cu wires: I=2×7 cm each; stirring rate=700 rpm. [b] Estimated from reference [14], in DMF at 25°C. [c] Calculated from ¹H NMR in CDCl₃ using DMF as internal standard. [d] Calculated as the slopes of ln([M]₀/[M]) ν s t plots. [e] Calculated from THF GPC with triple detector at T=30°C. [f] Calculated from ¹H NMR: M_n th=Conv.×DP× M_{MA} + M_{EBiB} . [g] D= M_w/M_n .



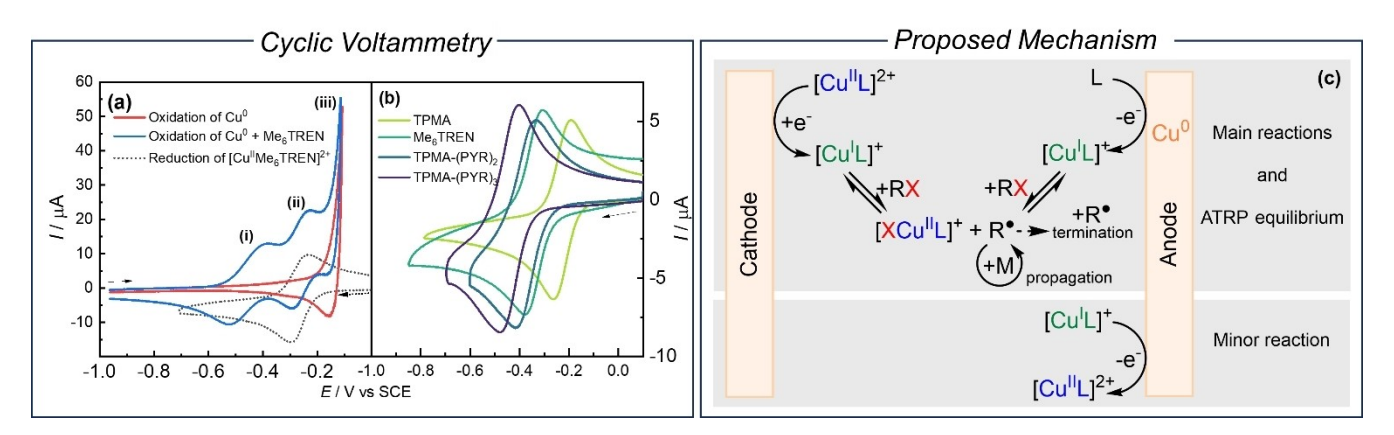


Figure 5. (a) Cyclic voltammetries in DMSO+0.1 M Et₄NBF₄ T = 25 °C and v = 0.2 V s⁻¹. Oxidation on Cu⁰ disk (d = 2 mm) with (blue line) and without (red line) 10⁻³ M Me₆TREN. Reduction of 10⁻³ M Cu^{II} trifluoromethanesulfonate/Me₆TREN on GC electrode. (b) Reduction of 5×10⁻⁴ M $[Br-Cu^{\parallel}L]^{2+}$ complexes recorded on a GC electrode. L is indicated in the legend. (c) Electrochemical reactions occurring at the electrodes during AC eATRP.

Without any amine ligand, a single sharp anodic peak at −0.1 V vs SCE oxidation signal was observed (iii), assigned to the oxidation of the electrode surface to Cu²⁺ (red line in Figure 5a).

Marked differences in the CV were observed under the conditions relevant for polymerization, i.e., in the presence of a ligand (Me6TREN in this case). Two new reversible peak couples arose upon oxidation (blue line in Figure 5a). The first peak couple (i) was associated with the monoelectronic (quasi)reversible oxidation of Cu⁰, with formation of the $[Cu^{I}L]^{+}$ complex, at halfwave potential $E_{1/2} = -0.453 \text{ V}$ vs SCE:

$$Cu^{0} + L = [Cu^{I}L]^{+} + e^{-}$$
(1)

The second peak couple (ii) was associated to the monoelectronic reversible oxidation of the ensuing Cu^I complex to $[Cu^{II}L]^{2+}$ with $E_{1/2} = -0.259 \text{ V } vs \text{ SCE}$:

$$[Cu^{I}L]^{+} = [Cu^{II}L]^{2+} + e^{-}$$
 (2)

To confirm the assignment of this second peak couple to reaction (2), we prepared the [CuIL]+ complex in situ by mixing Me6TREN with CuII trifluoromethanesulfonate and recorded its voltammogram in DMSO (dotted line in Figure 5a). The potential values of the reversible reduction of the [Cu^{II}L]⁺ complex perfectly overlapped with the peak couple (ii) recorded on the Cu⁰ electrode, confirming its assignment to the formation of [Cu^{II}L]⁺. The third and final sharp peak, when the potential at Cu⁰ was further swept towards positive values (up to 0 V vs SCE), was assigned the oxidation of bulk Cu⁰ to Cu²⁺. A similar pattern was observed for the oxidation of the Cu⁰ surface in the presence of both Me₆TREN and Br⁻ (Figure S22). From this electrochemical analysis, it is apparent that the Cu⁰ anode, under the mild oxidative current conditions applied in AC electrolysis in the presence of excess ligand, undergoes a gradual oxidation process to form the activator complex

[Cu^IL]⁺, while further oxidation to the Cu(II) deactivator is disfavored.

Additionally, the concentration of Cu species was monitored during AC polymerization via spectrochemical methods (Figure S26). Upon application of a current on Cu-Cu electrodes, very quick formation of soluble Cu species was observed, within half hour, resulting in fast polymerization. Conversely, very slow formation of soluble Cu species was observed without application of the electrochemical stimulus, resulting in slow polymerization by SARA ATRP (entry 8, Table 1). This phenomenon explains the fast and well-controlled polymerizations observed in AC eATRP with the Cu/Cu electrode pair.

Additionally, AC eATRP resulted in a lower final Cu(II) concentration. Since Cu(II) arises from biradical termination reactions, a low Cu(II) concentration is linked to good chain end fidelity and a low degree of radical termination.^[15]

An overall mechanism for AC eATRP is presented in Figure 5c. The main electrochemical reactions occurring at the electrode surfaces involve the reduction of the Cu(II) complex and the ligand-assisted oxidation the Cu surface. Both reactions generate the activator [Cu^IL]⁺. The oxidation of [Cu^IL]⁺ to the Cu(II) deactivator is a minor reaction.^[10d]

AC eATRP of MA with Catalysts of Different Activity

We conducted polymerizations of MA using different catalysts while maintaining a sinusoidal waveform. This approach was aimed at elucidating the impact of the catalyst on the process and assessing the general applicability of the AC electrosynthesis method. To vary the activity of the catalyst, the electron density of the amine ligand was tuned.[16] We thus synthesized para-substituted ligands with different activity by divergent chemistry, [17] starting from the 4-chloropyridine building block using the pyrrolidine EDGs (see Scheme S1). After complexation with Cu²⁺ in the presence of one equivalent of Br-, the four resulting [Br-Cu^{II}L]⁺ catalysts were analyzed by CV in DMSO (Figure 5b). All complexes revealed a reversible CV,

indicating the stability of corresponding Cu^I complexes. The introduction 2- or 3- pyrrolidine EDGs to the TPMA scaffold provoked a negative shift in the halfwave potential. The standard reduction potential (E°) of Cu/L complexes is crucial for predicting their performance as ATRP catalysts, with more negative E° values of $[X-Cu^{II}L]^{+}$ correlating with higher K_{ATRP} values. [7e,17-18] The activity of the catalysts, listed in Table 4, increased in the order TPMA < $Me_6TREN < TPMA-(PYR)_2 < TPMA-(PYR)_3$, with K_{ATRP} values rising by approximately one order of magnitude between each catalysts and by 2.5 orders of magnitude in total. These findings align with previous studies using DMF as the solvent.[17]

AC eATRP experiments were conducted with the four catalysts, as detailed in Table 4 and Figure S23. Faster polymerizations occurred using the two most active catalysts. The slowest catalyst, [Br-CuIITPMA]+, reached a plateau at 68 % conversion after 2 hours. In all cases, D was < 1.10.

Faster reactivity with highly active catalysts such as [Cu^ITPMA–(PYR)₃]⁺ or [Cu^ITPMA–(PYR)₂]⁺could be attributed to two reasons: (i) they may cause fewer termination side reactions; [19] (ii) they reacted quickly with the dormant PMA-Br alkyl halide before a polarity change, resulting in a very low Cu(I) surface concentration. This prevents oxidation back to the Cu(II) deactivators upon polarity change. To confirm this latter point, catalysts concentrations at the electrode surfaces have been estimated as described in Figure S25.

It is worth noting that [Cu^{II}TPMA–(PYR)₃]⁺ and [Cu^{II}TPMA-(PYR)₂]⁺ afforded nearly identical polymerizations of PMA-Br; however, TPMA-(PYR)2 is synthetically more accessible than TPMA-(PYR)3 because the primary amine 2-pycolylamine required for the synthesis is commercially available.

Conclusions

This work introduced AC electrolysis in electrochemically mediated ATRP, using various waveforms. Utilizing a symmetrical Cu⁰/Cu⁰ electrode pair, capitalizing on both comproportionation (SARA) and electrochemical regeneration, proved optimal for leveraging AC properties. An optimum pulse frequency range of 0.1 Hz was determined, with higher frequencies resulting in slower polymerizations.

A small alternating current generator was used to generate sinusoidal, triangular, or square waves. Square and sinusoidal waves yielded the best results. All polymerizations triggered by AC and pulsed electrolysis (0.1 Hz) were faster and yielded more controlled PMA-Br than a SARA ATRP performed under the same conditions but without the superimposed electrochemical stimulus. Highly active catalysts derived from para-substituted TPMA ligands were employed due to the rapid polarity changes induced by the alternating waveform. Pyridine-substituted catalysts performed the best and were most suitable for AC eATRP of MA.

AC eATRP was expanded to polymerize several different monomers, Remarkably, the same electrochemical stimulus (a $\pm 22 \,\mu\text{A}$ square wave triggered by the same Cu⁰ electrode pair) was effective under vastly different conditions including eleven monomers, six catalysts, three initiators, in various media including organic solvents, water, and bulk monomer. This setup overcomes the typical process optimization required in potentiostatic or galvanostatic eATRP. Additionally, reaction scale-up to 100 mL was achieved by rescaling currents while maintaining the same electrode pair. SEM analysis of the electrodes revealed minimal signs of corrosion after 15 consecutive experiments.

Chain extension experiments starting from macroinitiators produced by AC eATRP afforded the block copolymers PMETAC-b-POEOMA₅₀₀-Cl PNIPAM-b-PHEAAm-Br in water and PMA-b-PMA-Br in DMSO. This confirmed the high livingness of the polymers. This work demonstrates that AC electrolysis can effectively drive polymerization processes such as ATRP with a higher versatility than any other eATRP process previously reported.

Supporting Information

The authors have cited additional references within the Supporting Information.[19-28]

Author Contributions

F. D. B. conceived the idea and designed the experiments with M.F. and wrote the initial manuscript draft. F. D. B., V. P., T. L. B. performed the experiments and analyzed data. M. F. and F. D. B. supervised the work. F. D. B., M. F., J. F. J. C. and K. M. acquired funding. All authors discussed the results and contributed to the preparation and editing of the manuscript. All authors have agreed to the final version of the manuscript.

Acknowledgements

The authors acknowledge Dr. A. Doimo for his kind assistance in setting up the AC current generator, Giovanni Lissandrini for their kind help during the polymerizations and C. Patacas for the kind help with SEM imaging. F. D. B. thanks FCT-Fundaça o para a Ciencia e a Tecnologia (Portuguese Foundation for Science and Technology) for financial support through the grants POLYCEL (POCI-01-0145-FEDER-029742) and POLYELECTRON (PTDC/ EQU-EQU/2686/2020). V. A. P. thanks FCT for her PhD grant (SFRH/BD/138793/2018). M. F. thanks University of Padova, Stars Grant Stg-2021 "Photo-e-cat" for funding. K. M. acknowledges support from NSF (CHE 2401112). The ¹H NMR data were collected in part at the UC NMR facility which is supported in part by FEDER-European Regional Development Fund through the COMPETE Programme (Operational Programme for Competitiveness) and by Na-



tional Funds through FCT—Fundaca, o para a Ciencia e a Tecnologia (Portuguese Foundation for Science and Technology) through Grants REEQ/481/QUI/2006, RECI/QEQ-QFI/0168/2012, CENTRO-07-CT62-FEDER-002012, and Rede Nacional de Ressonancia Magnetica Nuclear (RNRMN). This research was partially sponsored by FED-ER funds through the program COMPETE—Programa Operacional Factores de Competitividade—and by national funds through FCT—Fundação para a Ciência e a Tecnologia, under the project UIDB/00285/2020 and LA/P/0012/2020. Open Access publishing facilitated by Università degli Studi di Padova, as part of the Wiley - CRUI-CARE agreement.

Conflict of Interest

The authors declare no conflict of interest.

Data Availability Statement

The data that support the findings of this study are available in the Supporting Information of this article.

Keywords: alternating current \cdot ATRP \cdot electrochemistry \cdot ligand design \cdot polymerization

- [1] S. Rodrigo, D. Gunasekera, J. P. Mahajan, L. Luo, Curr. Opin. Electrochem. 2021, 28, 100712.
- [2] a) D. Gunasekera, J. P. Mahajan, Y. Wanzi, S. Rodrigo, W. Liu, T. Tan, L. Luo, J. Am. Chem. Soc. 2022, 144, 9874–9882;
 b) K. Hayashi, J. Griffin, K. C. Harper, Y. Kawamata, P. S. Baran, J. Am. Chem. Soc. 2022, 144, 5762–5768.
- [3] L. Zeng, Y. Jiao, W. Yan, Y. Wu, S. Wang, P. Wang, D. Wang, Q. Yang, J. Wang, H. Zhang, A. Lei, *Nature Synthesis* 2023, 2, 172–181.
- [4] a) L. Lu, Y. Xie, Z. Yang, B. Chen, J. Hazard. Mater. 2023, 442, 130021; b) S. Rodrigo, C. Um, J. C. Mixdorf, D. Gunasekera, H. M. Nguyen, L. Luo, Org. Lett. 2020, 22, 6719–6723; c) D. Wang, T. Jiang, H. Wan, Z. Chen, J. Qi, A. Yang, Z. Huang, Y. Yuan, A. Lei, Angew. Chem. Int. Ed. Engl. 2022, 61, e202201543; d) J. S. Zhong, C. L. Ding, H. Kim, T. McCallum, K. Y. Ye, Green Synthesis and Catalysis 2022, 3, 4–10; e) L. E. Sattler, C. J. Otten, G. Hilt, Chemistry 2020, 26, 3129–3136.
- [5] L. Zeng, J. Wang, D. Wang, H. Yi, A. Lei, Angew. Chem. Int. Ed. Engl. 2023, 62, e202309620.
- [6] F. De Bon, F. Lorandi, J. F. J. Coelho, A. C. Serra, K. Matyjaszewski, A. A. Isse, *Chem. Sci.* 2022, 13, 6008–6018.
- [7] a) F. Lorandi, M. Fantin, K. Matyjaszewski, J. Am. Chem. Soc. 2022; b) K. Matyjaszewski, J. Xia, Chem. Rev. 2001, 101, 2921–2990; c) J.-S. Wang, K. Matyjaszewski, J. Am. Chem. Soc. 1995, 117, 5614–5615; d) S. Dworakowska, F. Lorandi, A. Gorczynski, K. Matyjaszewski, Adv. Sci. 2022, 9, e2106076; e) X. Pan, M. Fantin, F. Yuan, K. Matyjaszewski, Chem. Soc. Rev. 2018, 47, 5457–5490.
- [8] a) F. De Bon, R. G. Fonseca, F. Lorandi, A. C. Serra, A. A. Isse, K. Matyjaszewski, J. F. J. Coelho, *Chem. Eng. J.* 2022, 445, 136690; b) F. De Bon, M. Fantin, A. A. Isse, A. Gennaro, *Polym. Chem.* 2018, 9, 646–655; c) S. Park, P. Chmielarz, A. Gennaro, K. Matyjaszewski, *Angew. Chem. Int. Ed.* 2015, 54, 2388–2392; d) A. J. D. Magenau, N. Bortolamei, E. Frick, S.

- Park, A. Gennaro, K. Matyjaszewski, *Macromolecules* **2013**, *46*, 4346–4353; e) A. J. D. Magenau, N. C. Strandwitz, A. Gennaro, K. Matyjaszewski, *Science* **2011**, *332*, 81–84.
- [9] a) J. P. Mendes, J. R. Góis, J. R. C. Costa, P. Maximiano, A. C. Serra, T. Guliashvili, J. F. J. Coelho, J. Polym. Sci. Part A 2017, 55, 1322–1328; b) Y. Zhang, Y. Wang, K. Matyjaszewski, Macromolecules 2011, 44, 683–685; c) D. Konkolewicz, Y. Wang, P. Krys, M. Zhong, A. A. Isse, A. Gennaro, K. Matyjaszewski, Polym. Chem. 2014, 5, 4409; d) D. Konkolewicz, P. Krys, J. R. Góis, P. V. Mendonça, M. Zhong, Y. Wang, A. Gennaro, A. A. Isse, M. Fantin, K. Matyjaszewski, Macromolecules 2014, 47, 560–570; e) D. Konkolewicz, Y. Wang, M. J. Zhong, P. Krys, A. A. Isse, A. Gennaro, K. Matyjaszewski, Macromolecules 2013, 46, 8749–8772; f) C. M. R. Abreu, A. C. Serra, A. V. Popov, K. Matyjaszewski, T. Guliashvili, J. F. J. Coelho, Polym. Chem. 2013, 4, 5629–5636.
- [10] a) A. S. R. Oliveira, P. V. Mendonça, A. C. Serra, J. F. J. Coelho, J. Polym. Sci. 2019, 58, 145-153; b) R. Whitfield, A. Anastasaki, V. Nikolaou, G. R. Jones, N. G. Engelis, E. H. Discekici, C. Fleischmann, J. Willenbacher, C. J. Hawker, D. M. Haddleton, J. Am. Chem. Soc. 2017, 139, 1003-1010; c) A. Anastasaki, V. Nikolaou, D. M. Haddleton, Polym. Chem. 2016, 7, 1002-1026; d) K. F. Augustine, T. G. Ribelli, M. Fantin, P. Krys, Y. Cong, K. Matyjaszewski, J. Polym. Sci. Part A 2017, 55, 3048–3057; e) C. M. R. Abreu, L. Fu, S. Carmali, A. C. Serra, K. Matyjaszewski, J. F. J. Coelho, Polym. Chem. 2017, 8, 375-387; f) J. P. Mendes, P. V. Mendonca, P. Maximiano, C. M. R. Abreu, T. Guliashvili, A. C. Serra, J. F. J. Coelho, RSC Adv. 2016, 6, 9598-9603; g) P. Krys, Y. Wang, K. Matyjaszewski, S. Harrisson, Macromolecules 2016, 49, 2977-2984; h) P. Chmielarz, P. Krys, S. Park, K. Matyjaszewski, Polymer 2015, 71, 143-147; i) J. P. Mendes, F. Branco, C. M. Abreu, P. V. Mendonca, A. V. Popov, T. Guliashvili, A. C. Serra, J. F. Coelho, ACS Macro Lett. 2014, 3, 544-547.
- [11] S. Dadashi-Silab, K. Matyjaszewski, Macromolecules 2018, 51, 4250–4258.
- [12] A. J. Rieth, M. I. Gonzalez, B. Kudisch, M. Nava, D. G. Nocera, J. Am. Chem. Soc. 2021, 143, 14352–14359.
- [13] M. Fantin, F. Lorandi, A. A. Isse, A. Gennaro, *Macromol. Rapid Commun.* 2016, 37, 1318–1322.
- [14] F. Lorandi, M. Fantin, H. Jafari, A. Gorczynski, G. Szczepaniak, S. Dadashi-Silab, A. A. Isse, K. Matyjaszewski, J. Am. Chem. Soc. 2023, 145, 21587–21599.
- [15] P. Krys, K. Matyjaszewski, Eur. Polym. J. 2017, 89, 482-523.
- [16] F. Lorandi, K. Matyjaszewski, Isr. J. Chem. 2019, 60, 108-123.
- [17] A. E. Enciso, F. Lorandi, A. Mehmood, M. Fantin, G. Szczepaniak, B. G. Janesko, K. Matyjaszewski, *Angew. Chem. Int. Ed. Engl.* 2020, 59, 14910–14920.
- [18] a) T. G. Ribelli, M. Fantin, J.-C. Daran, K. F. Augustine, R. Poli, K. Matyjaszewski, J. Am. Chem. Soc. 2018, 140, 1525–1534; b) F. Lorandi, F. De Bon, M. Fantin, A. A. Isse, A. Gennaro, Electrochem. Commun. 2017, 77, 116–119; c) P. Chmielarz, M. Fantin, S. Park, A. A. Isse, A. Gennaro, A. J. D. Magenau, A. Sobkowiak, K. Matyjaszewski, Prog. Polym. Sci. 2017, 69, 47–78; d) M. Fantin, A. A. Isse, N. Bortolamei, K. Matyjaszewski, A. Gennaro, Electrochim. Acta 2016, 222, 393–401
- [19] G. Xie, M. R. Martinez, W. F. M. Daniel, A. N. Keith, T. G. Ribelli, M. Fantin, S. S. Sheiko, K. Matyjaszewski, *Macro-molecules* 2018, 51, 6218–6225.
- [20] a) A. E. Enciso, F. Lorandi, A. Mehmood, M. Fantin, G. Szczepaniak, B. G. Janesko, K. Matyjaszewski, *Angew. Chem. Int. Ed. Engl.* 2020, 59, 14910–14920; b) K. Schroder, R. T. Mathers, J. Buback, D. Konkolewicz, A. J. D. Magenau, K. Matyjaszewski, *ACS Macro Lett.* 2012, 1, 1037–1040.
- [21] a) T. G. Ribelli, M. Fantin, J.-C. Daran, K. F. Augustine, R. Poli, K. Matyjaszewski, J. Am. Chem. Soc. 2018, 140, 1525–



5213773, 2024, 29, Downloaded from https://onlinelibitary.wiley.com/doi/10.1002/anic.202406484 by Carnegie Mellon University, Wiley Online Library on [03/06/2025], See the Terms and Conditions (https://onlinelibitary.wiley.com/rerms-and-conditions) on Wiley Online Library for rules of use; OA articles are governed by the applicable Creative Commons

- 1534; b) X. Pan, M. Fantin, F. Yuan, K. Matyjaszewski, *Chem. Soc. Rev.* 2018, 47, 5457–5490; c) F. Lorandi, F. De Bon, M. Fantin, A. A. Isse, A. Gennaro, *Electrochem. Commun.* 2017, 77, 116–119; d) P. Chmielarz, M. Fantin, S. Park, A. A. Isse, A. Gennaro, A. J. D. Magenau, A. Sobkowiak, K. Matyjaszewski, *Prog. Polym. Sci.* 2017, 69, 47–78; e) M. Fantin, A. A. Isse, N. Bortolamei, K. Matyjaszewski, A. Gennaro, *Electrochim. Acta* 2016, 222, 393–401.
- [22] W. A. Braunecker, N. V. Tsarevsky, A. Gennaro, K. Matyjaszewski, *Macromolecules* 2009, 42, 6348–6360.
- [23] a) A. E. Enciso, F. Lorandi, A. Mehmood, M. Fantin, G. Szczepaniak, B. G. Janesko, K. Matyjaszewski, *Angew. Chem. Int. Ed. Engl.* 2020, 59, 14910–14920; b) K. Schroder, R. T. Mathers, J. Buback, D. Konkolewicz, A. J. D. Magenau, K. Matyjaszewski, *ACS Macro Lett.* 2012, 1, 1037–1040.
- [24] M. Alimi, A. Allam, M. Selkti, A. Tomas, P. Roussel, E. Galardon, I. Artaud, *Inorg. Chem.* 2012, 51, 9350–9356.
- [25] a) T. G. Ribelli, M. Fantin, J.-C. Daran, K. F. Augustine, R. Poli, K. Matyjaszewski, J. Am. Chem. Soc. 2018, 140, 1525–

- 1534; b) X. Pan, M. Fantin, F. Yuan, K. Matyjaszewski, *Chem. Soc. Rev.* 2018, 47, 5457–5490; c) F. Lorandi, F. De Bon, M. Fantin, A. A. Isse, A. Gennaro, *Electrochem. Commun.* 2017, 77, 116–119; d) P. Chmielarz, M. Fantin, S. Park, A. A. Isse, A. Gennaro, A. J. D. Magenau, A. Sobkowiak, K. Matyjaszewski, *Prog. Polym. Sci.* 2017, 69, 47–78; e) M. Fantin, A. A. Isse, N. Bortolamei, K. Matyjaszewski, A. Gennaro, *Electrochim. Acta* 2016, 222, 393–401.
- [26] W. A. Braunecker, N. V. Tsarevsky, A. Gennaro, K. Matyjaszewski, *Macromolecules* 2009, 42, 6348–6360.
- [27] G. Gazzola, A. Antonello, A. A. Isse, M. Fantin, ACS Macro Lett. 2023, 1602–1607.
- [28] M. S. Alam, B. Ashokkumar, A. M. Siddiq, J. Mol. Liq. 2019, 281, 584–597.

Manuscript received: April 5, 2024 Accepted manuscript online: April 22, 2024 Version of record online: June 14, 2024